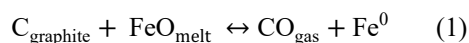


**CARBON AS A KEY DRIVER OF EXPLOSIVE VOLCANISM ON MERCURY.** <sup>1</sup>K. Iacovino, <sup>2</sup>F. M. McCubbin, <sup>3</sup>K. E. Vander Kaaden, <sup>1</sup>G. M. Moore, <sup>1</sup>Jacobs/NASA Johnson Space Center (email: kayla.iacovino@nasa.gov), Houston, TX, <sup>2</sup>NASA Johnson Space Center, Houston, TX, <sup>3</sup>NASA Headquarters, Washington, D.C.

**Explosive volcanism on Mercury:** To date, 150 candidate sites of explosive volcanism have been identified on Mercury, each consisting of endogenic pits surrounded by relatively bright, diffuse, and spectrally “red” deposits [1]. These deposits are interpreted to be pyroclastic in origin (generated by explosive volcanism) and vary in size with radii from 1.8–110.8 km [1]. The explosivity of any eruption depends upon the presence of volatiles (primarily H-C-O-S species) in the system. These volatiles may be sourced from the magma itself (as volatiles dissolved in silicate melt) or from an external source (e.g., a volatile-bearing deposit). In either case, explosive eruptions are driven by rapid expansion of volatiles as they change state (e.g., exsolution from silicate melt into gas bubbles, liquid to gas, or solid to gas).

Given the low solubilities of O-bearing species in reduced magmas in the H-C-O-S system, some external volatile source may be required to explain deposits observed on Mercury [2], which has an estimated surface oxygen fugacity of IW-3 to -7. Mercury contains abundant near-surface graphite-rich deposits, thought to be relics of a global graphite flotation crust [3], providing a potential reservoir for carbon, which could be converted to CO gas via interaction with silicate melt (i.e., smelting). Smelting has previously been proposed as a mechanism for explosive volcanism on the Moon [4] and recently on Mercury [2,5] via the reaction:



Recent experimental work on Mercury analog melts demonstrated that  $\leq 5$  wt% FeO ( $>95\%$  of the FeO in the melt) will participate in graphite-melt smelting requiring  $<1$  wt% graphite and producing  $\sim 2$  wt% CO gas [2].

**Drivers of eruption:** The production of CO gas dramatically increases the buoyancy of the system (magma + gas), which increases its ascent speed. During ascent, adiabatic expansion of fluid bubbles drives further buoyancy and ascent. This results in high eruption velocities, which are proportional to the concentration of volatiles in the system [6], along with explosive fragmentation of magma into solid ash particles. We can combine the equation relating deposit radius to initial ejection velocity on an airless body [6] and that relating ejection velocity to released volatile

gas fraction [7] into a generalized equation relating deposit radius,  $X$ , in meters to released volatile mass fraction of a particular gas species,  $n$ , in wt%:

$$n = \frac{gXm(\gamma-1)}{20RT\gamma} \quad (2)$$

Where  $g$  is the gravitational acceleration of the body in  $\text{m}\cdot\text{s}^{-2}$  ( $3.7 \text{ m}\cdot\text{s}^{-2}$  on Mercury),  $m$  is the molecular weight of the gas species in  $\text{g}\cdot\text{mol}^{-1}$ ,  $\gamma$  is the specific heat ratio ( $C_p/C_v$ ) of the gas at the temperature of interest,  $R$  is the gas constant  $8.3145 \text{ J}\cdot\text{mol}^{-1}\cdot\text{K}^{-1}$ , and  $T$  is the temperature in K.

Here we investigate the role of smelting in addition to possible contributions from magmatic degassing of H-C-O-S species given known solubility limits. Each species will contribute proportionally to the total released volatile fraction. We can write a generalized equation to solve for the volatile gas fraction of a mixed gas as:

$$n_{\text{Tot}} = \frac{gX}{20RT} \cdot \sum W_i \left( \frac{m_i(\gamma_i-1)}{\gamma_i} \right) \quad (3)$$

Where  $n_{\text{Tot}}$  is the sum total of released volatile fractions for each gas,  $i$ , in wt%,  $m_i$  is the molecular weight,  $\gamma_i$  is the specific heat ratio, and  $W_i$  is the weight fraction of gas  $i$  in the total gas.

For the case of graphite-induced smelting, we can also calculate the mass fraction of FeO in the melt required to produce any amount of gas and thus any deposit radius. The relationship between deposit radius, required graphite and FeO, and subsequent gas release is shown in Fig 1. Smelting of 5 wt% FeO alone can account for  $\sim 75\%$  pyroclastic deposits on Mercury (green box in Fig 1) but is insufficient to explain the largest deposits ( $>21$  km). An averaged sized mercurian pyroclastic deposit with a radius of 17.2 km requires 1.57 wt% CO. This volatile release would require  $\sim 7000$  ppm C. C solubility in extraterrestrial basalts is on the order of 10–100’s of ppm around IW-2 to IW-5 [8], with the lowest values corresponding to H-poor systems. Thus, outgassing of magmatic C is insufficient as a driver of explosive volcanism for any but the smallest of identified deposits ( $<3$  km).

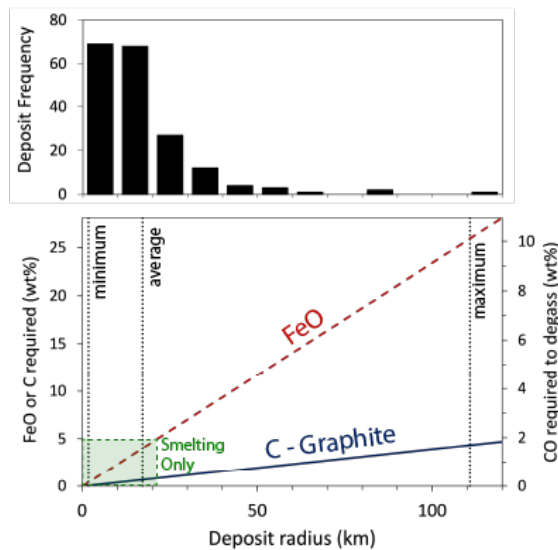


**Figure 1.** Top: size frequency of identified pyroclastic deposits on Mercury in deposit radius [1]. Bottom: relationship between deposit radius, graphite and FeO required for smelting, and produced CO gas. Vertical dotted lines represent minimum (1.8 km), average (17.2 km) and maximum (110.8 km) deposit sizes. The green box indicates the gas produced by the smelting of 5 wt% FeO [2].

**Thermodynamic modeling:** Next, we apply the thermodynamic model employed in [2] to predict the composition of magmatic gas that could be released from Mercurian melt in the system CO-CO<sub>2</sub>-H<sub>2</sub>-H<sub>2</sub>O-H<sub>2</sub>S-O<sub>2</sub>-S<sub>2</sub>-SO<sub>2</sub> at 1 bar, 1400 °C, and  $f_{O_2}$  at IW-4.5. Within the set of all possible gas compositions, we then use solubility constraints to narrow down the range of plausible dissolved volatile contents necessary to drive the largest pyroclastic deposits on Mercury. We assume maximum dissolved volatile concentrations of 1000 ppm total C [8], 5 wt% total S [9], and 3000 ppm total H [10].

Fig 2 shows all plausible dissolved volatile compositions that could produce pyroclastic deposits with radii  $\leq 17.2$  (planetary average),  $\leq 60$  km, and  $\leq 110.8$  (maximum) from: 1. magmatic degassing alone (without smelting; top); or 2. magmatic degassing in addition to smelting (bottom). In any case, the extremely low solubility of carbon in reduced silicate melts drives plausible dissolved volatile compositions toward the H-S binary. Without smelting, the range of compositions necessary to create average size deposits is extremely limited and requires either H-rich or S-rich gas. Larger deposits  $\leq 60$  km in radius are even more constrained, requiring a pure-H gas without smelting or a nearly pure-H or pure-S gas with smelting. With smelting, H-rich magmatic gas can account for all

deposits on Mercury except for the single largest deposit, Nathair Facula.

The high concentration of sulfur on the mercurian surface has led to the hypothesis that sulfur degassing may drive explosive volcanism, but this is only possible in the most refractory terrains where S solubility is enhanced. Thus, our results indicate that exsolution of magmatic volatiles alone is implausible as a driver of explosive volcanism on Mercury and suggest that, with or without smelting, H may play an important role particularly in less refractory terrains such as *Borealis Planitia*.

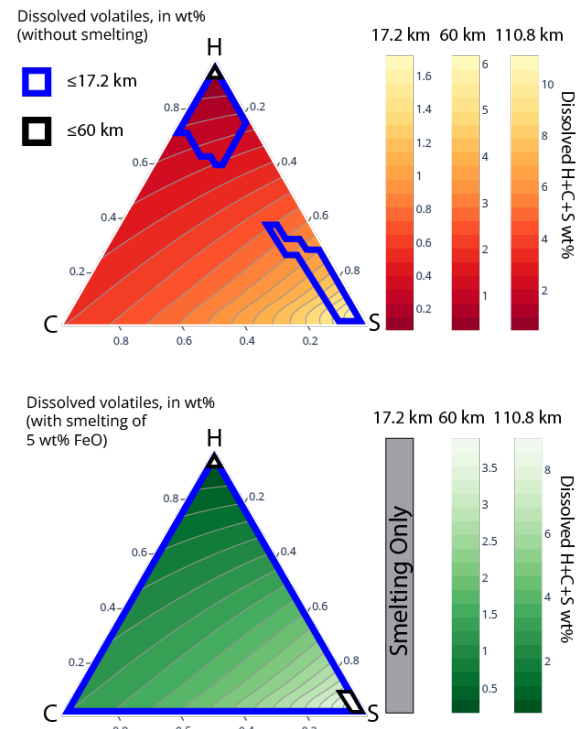


**Figure 2.** Ternaries showing dissolved H, C, or S in wt% required to produce deposit sizes of 17.2, 60, and 110.8 km, assuming volatiles sourced only from the magma (top) or magma plus smelting (bottom). Overlain blue and black bordered regions indicate dissolved H-C-S concentrations in wt% that could produce deposits  $\leq 17.2$  and  $\leq 60$  km assuming solubility limits.

**References:** [1] Thomas R. J. et al. (2014) *Icarus* 277. [2] Iacovino K. et al. (2023) *EPSL* 602. [3] Vander Kaaden K. E. and McCubbin F. M. (2015) *GCA* 149. [4] Fogel R. A. and Rutherford M. J. (1995) *GCA* 59. [5] McCubbin F. M. (2017) *JGR:P* 122. [6] Wilson L. (1980) *JVGR* 8. [7] Wilson L. et al. (2014) *LPSC* 45. [8] Li Y. et al. (2017) *JGRP* 122. [9] Namur O. et al. (2016) *EPSL* 448. [10] Hirschmann M. M. et al. (2012) *EPSL* 345.